The International Journal of Energy & Engineering Sciences, 2021, 6 (2) 23-37
ISSN: 2602-294X - Gaziantep University

IMPROVEMENT OF AERODYNAMIC PERFORMANCE OF AN AIRCRAFT USING MORPHING WING

İbrahim Göv[1*], Mehmet Hanifi Doğru[2], and Ümit Korkmaz[3]

[1*]Aerospace Engineering Department, Aeronautics and Aerospace Faculty, Gaziantep University, Gaziantep, Turkey
[2]Pilotage Department, Aeronautics and Aerospace Faculty, Gaziantep University, Gaziantep, Turkey
[3]Aerospace Engineering Department, Aeronautics and Aerospace Faculty, Gaziantep University, Gaziantep, Turkey

*igov@gantep.edu.tr

ABSTRACT

The aerodynamic performance of an aircraft directly affects the operating cost of the aircraft. The aerodynamic performance can be defined as the Cl/Cd ratio. To decrease operating costs Cl/Cd ratio must be increased. The main factor affecting the Cl/Cd ratio is the airfoil. Hence in this study, focused on a morphing airfoil during the flight to obtain maximum Cl/Cd ratio at various angle of attack values. 2D CFD analysis is used in this study based on NACA63-215 airfoil and a new NACA63-215_1 airfoil which is modified NACA63-215. In analyses, Cl/Cd ratio and flow separation were investigated as the performance parameters. At the end of the study, it was seen that the NACA63-215 airfoil should be used between 11^0-17^0 angle of attack, NACA63-215_1 should be used between 0^0-10^0, 18^0-23^0 angle of attack, to obtain maximum performance.

Keywords: Morphing Airfoil, flow separation, lift coefficient, drag coefficient

1. INTRODUCTION

A wing is a surface used to move through the air medium to generate an aerodynamic force normal to the direction of travel (Figure 1). Blades are systems with different profile structures used to generate lift force. Expressed as the ratio of lift coefficients (Cl) and drag coefficients (Cd), aerodynamic performance (AP) can be 60 or more in some gliders. This means that a small thrust force will be sufficient to obtain the lift force [1].

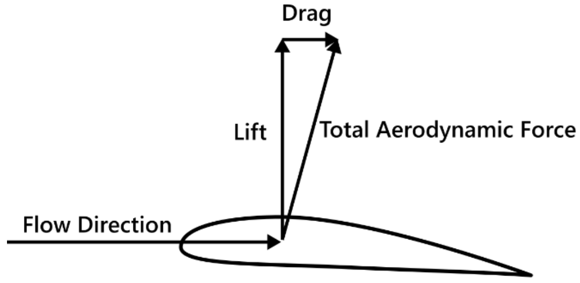

Figure 1. Aerodynamic forces

The performance of an aircraft wing is often impaired by the stall. The reason for the loss of flow on the wing profile surface is associated with the shapes of the wing profile. When the literature is examined, it is observed that there are many different studies about the AP of airfoils [2, 3, 4, 5, 6, 7, 8, 9, 10, 11,12, 13, and 14].

Standard wings are designed to provide maximum performance in a limited range of angles of attack (AoA). In the literature, it is seen that the performances of the standard profiles rapidly decrease outside of this range. It has been determined that different wing profiles are needed to improve this range at various AoA during the flight. At the end of the literature review, the use of variable airfoil during the flight was not encountered. For this reason, in the study, the use of a different wing profile was developed by changing the airfoil during flight. It was investigated to increase the AP of NACA63-215 at various angle of attack values.

2. METHOD OF ANALYSIS

In the performance of an airplane wing; Runway distance, approach speed, climb speed, load capacity, and operating range are known to have a significant effect. At the same time, it is known that an effective conveying system to be used causes a significant decrease in noise and emission levels as it reduces the thrust requirements. [15]

$$C_D=\frac{F_D}{\frac{1}{2}\rho v^2 A} \quad (1)$$

$$C_L=\frac{F_L}{\frac{1}{2}\rho v^2 A} \quad (2)$$

where F_D: Drag force, F_L: Lift force, v: Velocity, ρ: Density, and A: Effective area.

The Spalart-Allmaras turbulence model (equation 3-9) was used in CFD analysis of the 2D flow on the wing profiles. It is known that the Spalart-Allmaras turbulence model is an equation model specially designed for aerospace applications. [16]

$$\frac{\delta}{\delta t}(\rho\tilde{v}) + \frac{\delta}{\delta x_i}(p\tilde{v}u_i) = G_v + \frac{1}{\sigma_{\tilde{v}}}\left[\frac{\delta}{\delta x_j}\left\{(\mu + \rho\tilde{v})\frac{\delta\tilde{v}}{\delta x_j}\right\} + C_{b2}\rho\left(\frac{\delta\tilde{v}}{\delta x_j}\right)^2\right] - Y_v + S_{\tilde{v}} \quad (3)$$

$$\mu_t = \rho\tilde{v}f_{v1} \quad (4)$$

$$G_v = C_{b1}\rho\tilde{S}\tilde{v} \quad (5)$$

$$\tilde{S} \equiv S + \frac{\tilde{v}}{K^2 d^2} f_{v^2} \quad (6)$$

$$S \equiv \sqrt{2\Omega_{ij}\Omega_{ij}} \quad (7)$$

$$\Omega_{ij} = \frac{1}{2}\left(\frac{\delta u_i}{\delta x_j} - \frac{\delta u_j}{\delta x_i}\right) \quad (8)$$

$$Y_v = C_{w1}\rho f_w \left(\frac{\tilde{v}}{d}\right)^2 \quad (9)$$

Here, Cl value, Cd value, and flow separation (FS) of NACA63-215 and NACA63-215_1 (in Figure 2) are investigated. Analysis parameters are taken as steady-state, Spalart-Allmaras model, 1m/s inlet velocity (in order to comparison), 1m chord length.

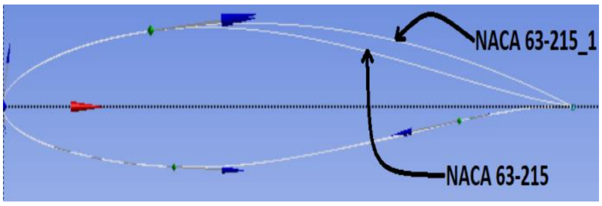

Figure 2. NACA63-215 and Improved Airfoil Profile

Analyses were performed using the FEA program ANSYS. The mesh model designed for the whole system is shown in Figure 3 with 30272 node numbers and 29920 element numbers. The detailed mesh model of NACA63-215 and improved airfoil is shown in Figure 4.

The International Journal of Energy & Engineering Sciences, 2021, 6 (2) 23-37
ISSN: 2602-294X - Gaziantep University

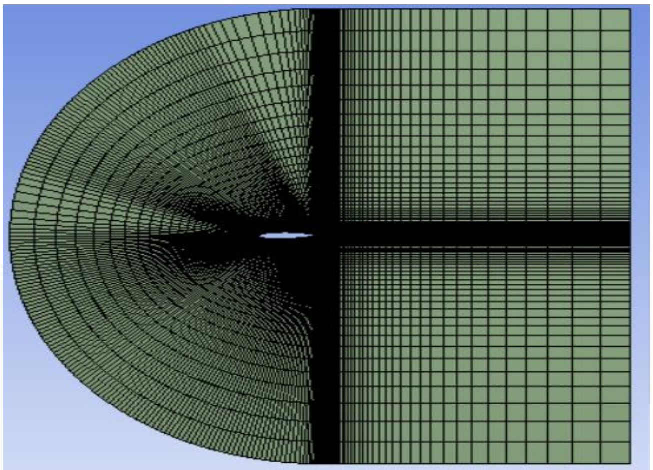

Figure 3. Complete mesh

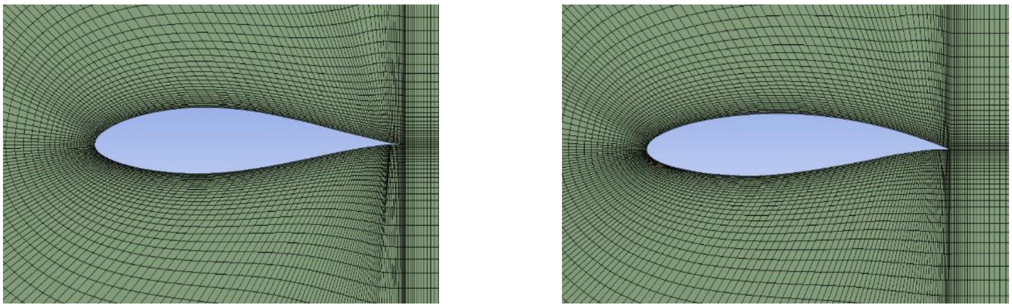

a) NACA63-215 b) NACA63-215_1

Figure 4. Enlarged view of NACA63-215 and improved NACA63-215_1 mesh

3. ANALYSIS

A comparison of the Cl results of Xfoil and ANSYS at 5^0 AoA value and 50000 Reynolds numbers are given in Figure 5. And the comparison of the Cd results of Xfoil and ANSYS at 5^0 AoA value and 50000 Reynolds numbers are given in Figure 6 [17].

The International Journal of Energy & Engineering Sciences, 2021, 6 (2) 23-37
ISSN: 2602-294X - Gaziantep University

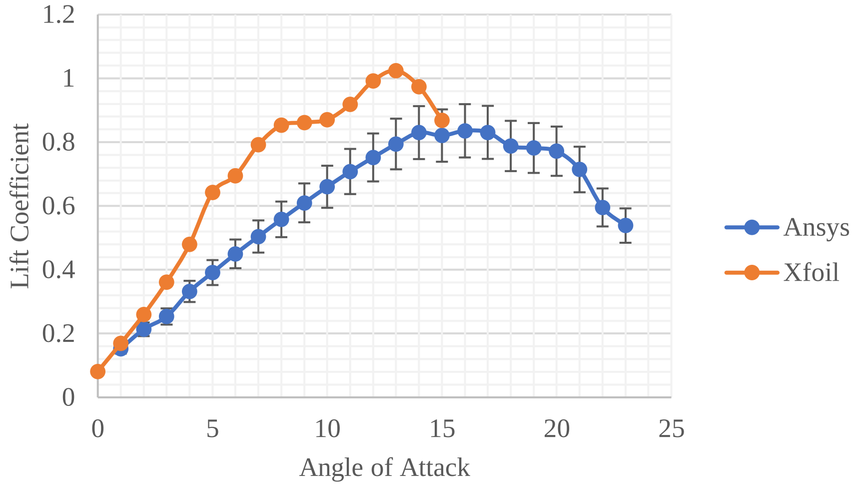

Figure 5. The Cl values according to Xfoil and ANSYS [17]

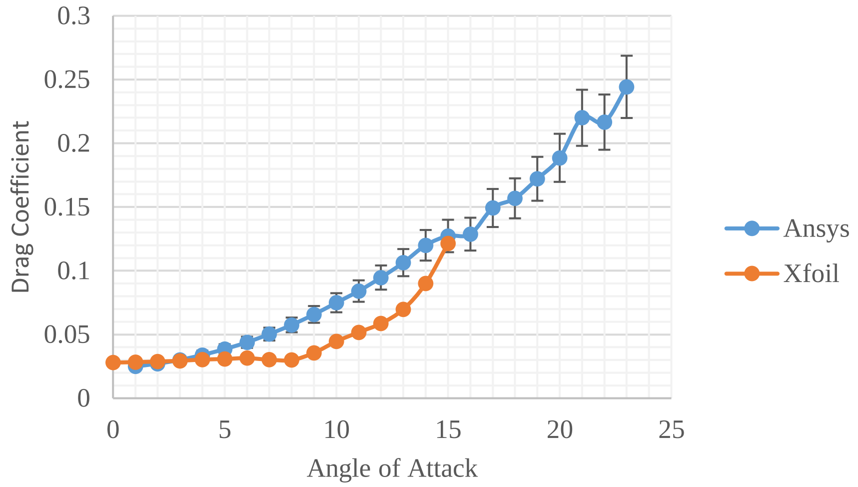

Figure 6. The Cd according to Xfoil and ANSYS [17]

After a comparison of Xfoil and Ansys results, the AP of the NACA63-215 and improved NACA63-215 airfoil (Figure 7) were compared. The AP of these 2-airfoils was compared at various AoA (between 0^0 and 23^0) values. CD, Cl, and FS were used as performance parameters. Analyses were performed at 7,0388 $\times 10^4$ Reynolds numbers.

Cl of NACA63-215 and NACA63-215_1 at the various angle of attack was given in Figure 7. Also, Cd of NACA63-215 and NACA63-215_1 at the various angle of attack was given in Figure 8.

When Figure 7 was investigated, it was seen that the maximum Cl was obtained at 17^0 angles of attack for original NACA63-215 and the minimum Cl was obtained at 0^0 angle of attack for original NACA63-215. Also, the maximum Cl was obtained at 21^0 angle of attack for NACA63-215_1 and the minimum Cl was obtained at 0^0 angle of attack for NACA63-215_1. So, comparisons of the results were given at these 3 angles of attack values.

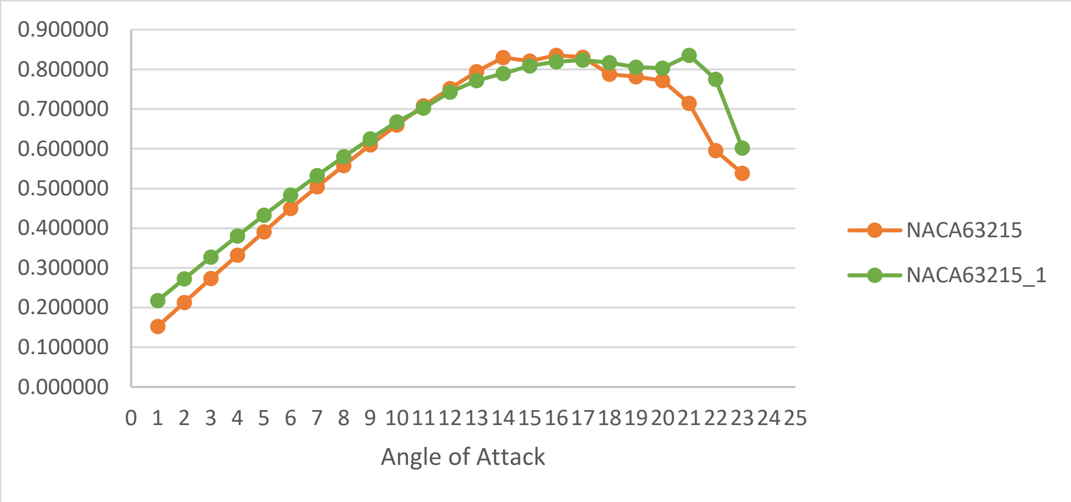

Figure 7. Cl at various AoA

The NACA63-215 airfoil should be used between 11^0-17^0 angle of attack, NACA63-215_1 should be used between 0^0-10^0, 18^0-23^0 angle of attack, to obtain maximum lift.

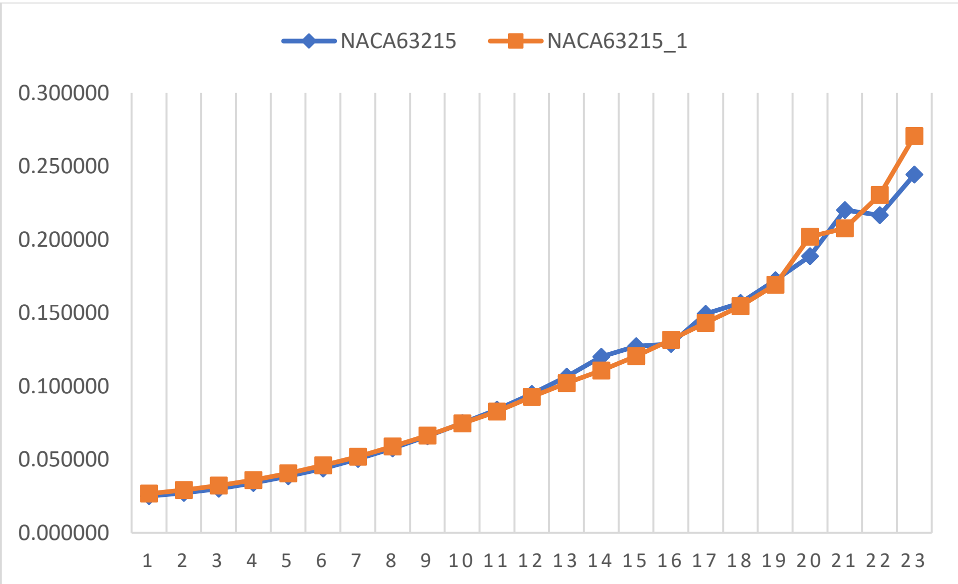

Figure 8. Cd at various AoA

There is no significant difference in terms of drag values between NACA63-215 and NACA63-215_1 at all angles of attack as shown in Figure 8.

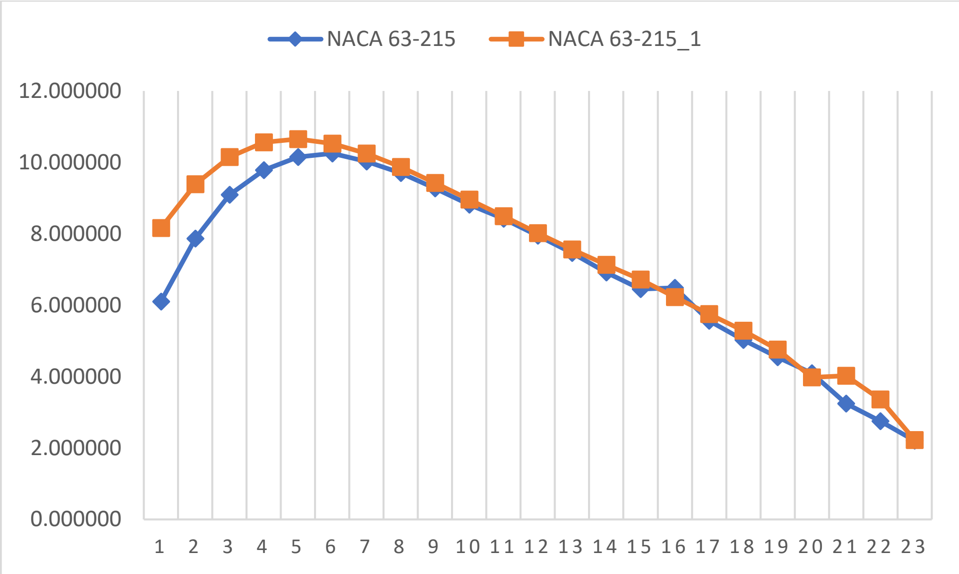

Figure 9. Cl/Cd at various AoA

Cl/Cd ratio was given according to the angle of attack in Figure 9. The NACA63-215_1 should be used all AoA to obtain maximum aerodynamic efficiency.

The pressure of NACA63-215 and NACA63-215_1 at 0^0 AoA values were given in Figures 10 and 11 respectively. The velocity of NACA63-215 and NACA63-215_1 at 0^0 AoA values were given in Figures 12 and 13 respectively.

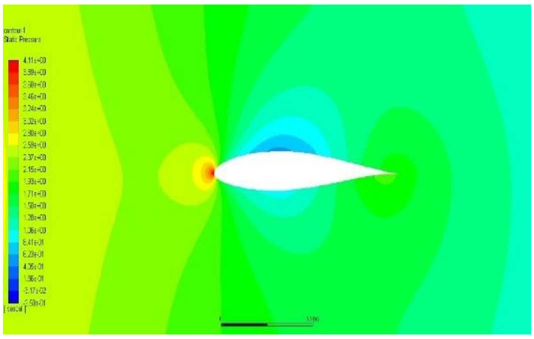

Figure 10. Pressure of NACA63-215 at 0^0 AoA

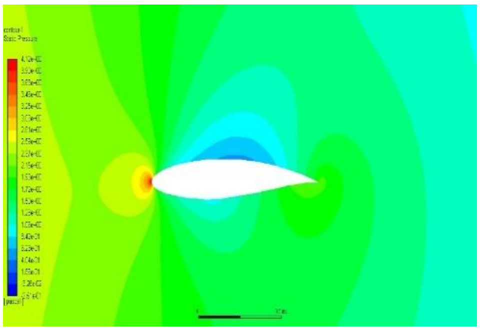

Figure 11. Pressure of NACA63-215_1 at 0^0 AoA

The International Journal of Energy & Engineering Sciences, 2021, 6 (2) 23-37
ISSN: 2602-294X - Gaziantep University

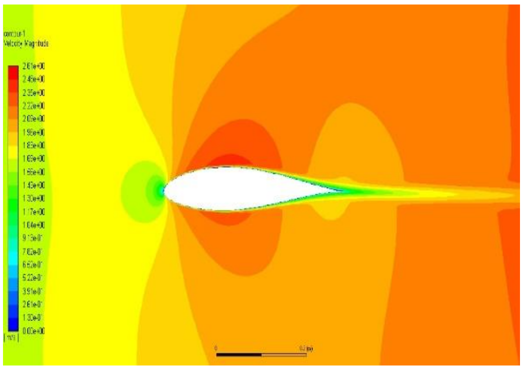

Figure 12. Velocity of NACA63-215 at 0^0 AoA

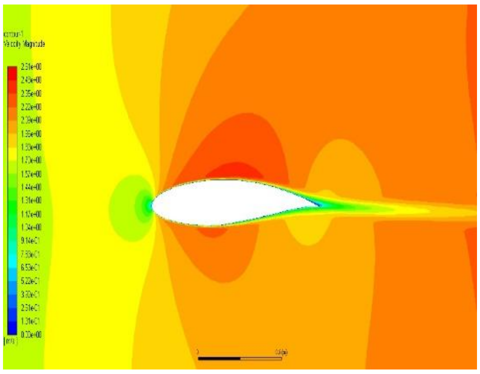

Figure 13. Velocity of NACA63-215_1 at 0^0 AoA

The pressure of NACA63-215 and NACA63-215_1 at 17^0 AoA values were given in Figures 14 and 15 respectively. The velocity of NACA63-215 and NACA63-215_1 at 17^0 AoA values were given in Figures 16 and 17 respectively.

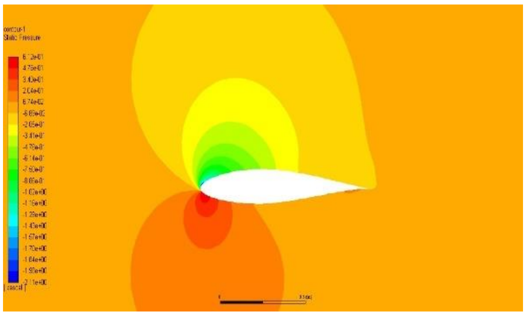

Figure 14. Pressure of NACA63-215 at 17^0 AoA

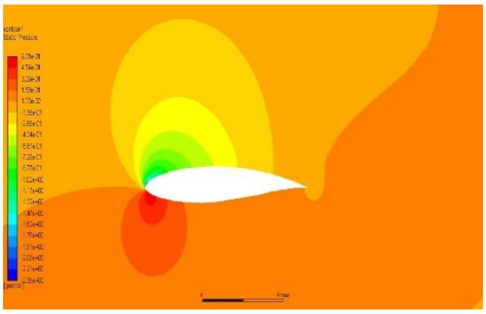

Figure 15. Pressure of NACA63-215_1 at 17^0 AoA

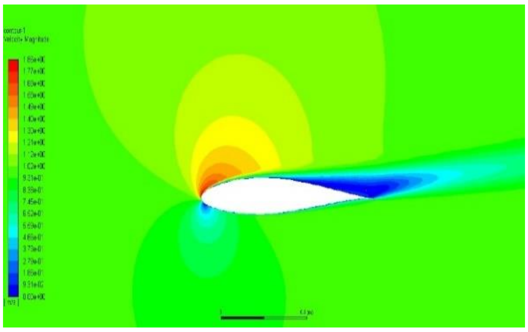

Figure 16. Velocity of NACA63-215 at 17^0 AoA

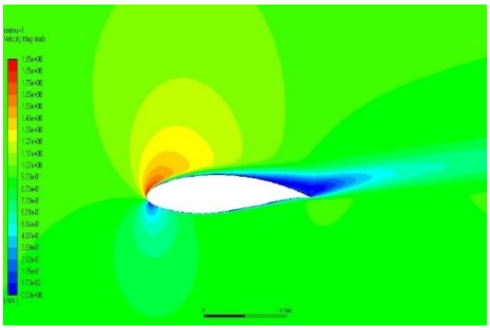

Figure 17. Velocity of NACA63-215_1 at 17^0 AoA

The pressure of NACA63-215 and NACA63-215_1 at 21^0 AoA values were given in Figures 18 and 19 respectively. The velocity of NACA63-215 and NACA63-215_1 at 21^0 AoA values were given in Figures 20 and 21 respectively.

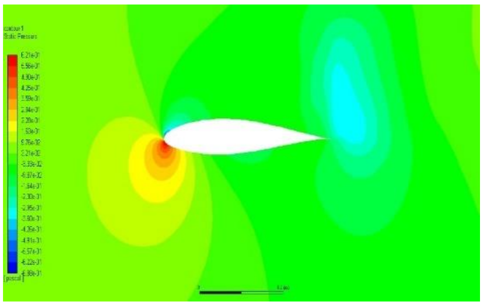

Figure 18. Pressure of NACA63-215 at 21^0 AoA

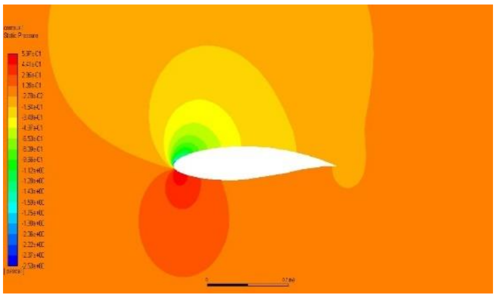

Figure 19. Pressure of NACA63-215_1 at 21^0 AoA

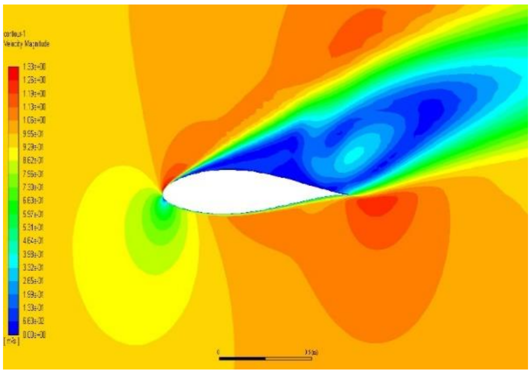

Figure 20. Velocity of NACA63-215 at 21^0 AoA

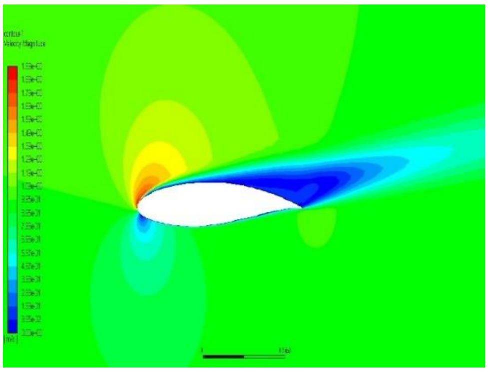

Figure 21. Velocity of NACA63-215_1 at 21^0 AoA

The velocity vector of NACA63-215 and NACA63-215_1 0^0 AoA values was given in Figures 22 and 23 respectively.

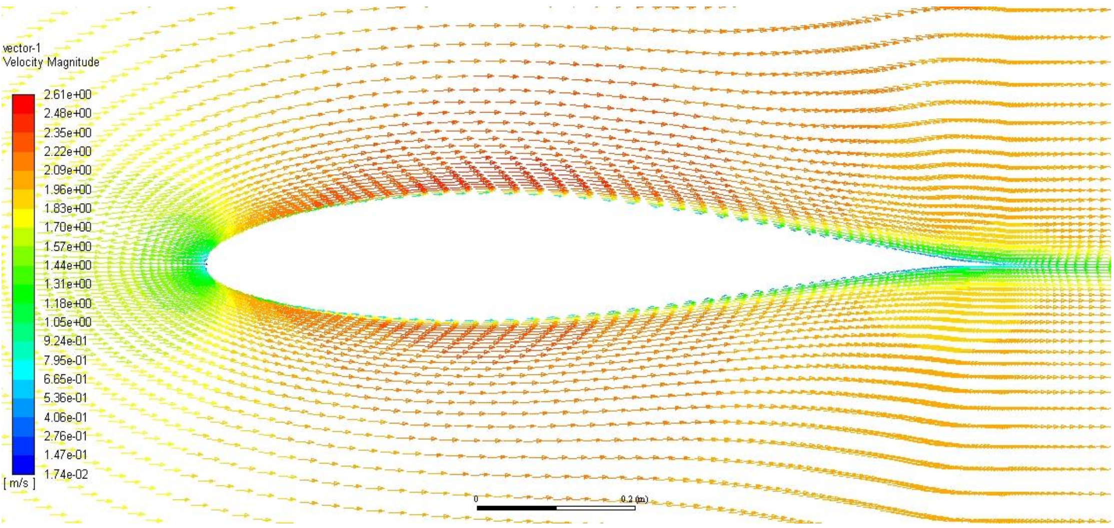

Figure 22. Velocity vector of NACA63-215 at 0^0 AoA

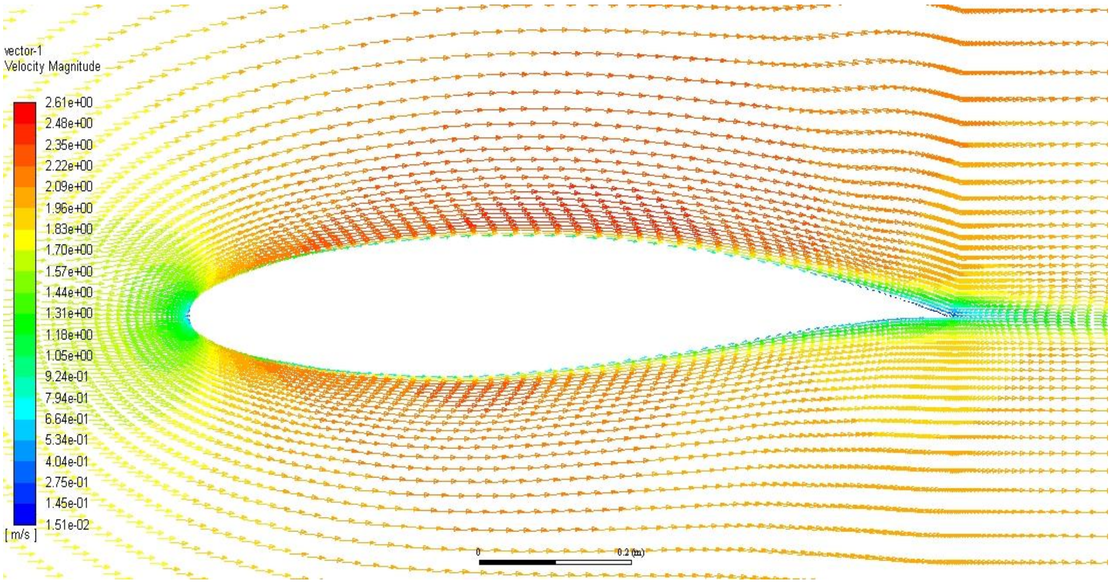

Figure 23. Velocity vector of NACA63-215_1 at 0^0 AoA

When Figures 22 and 23 were investigated it was seen that there was no FS at 0^0 AoA.

The velocity vector of NACA63-215 and NACA63-215_1 at 17^0 AoA values were given in Figures 24 and 25 respectively.

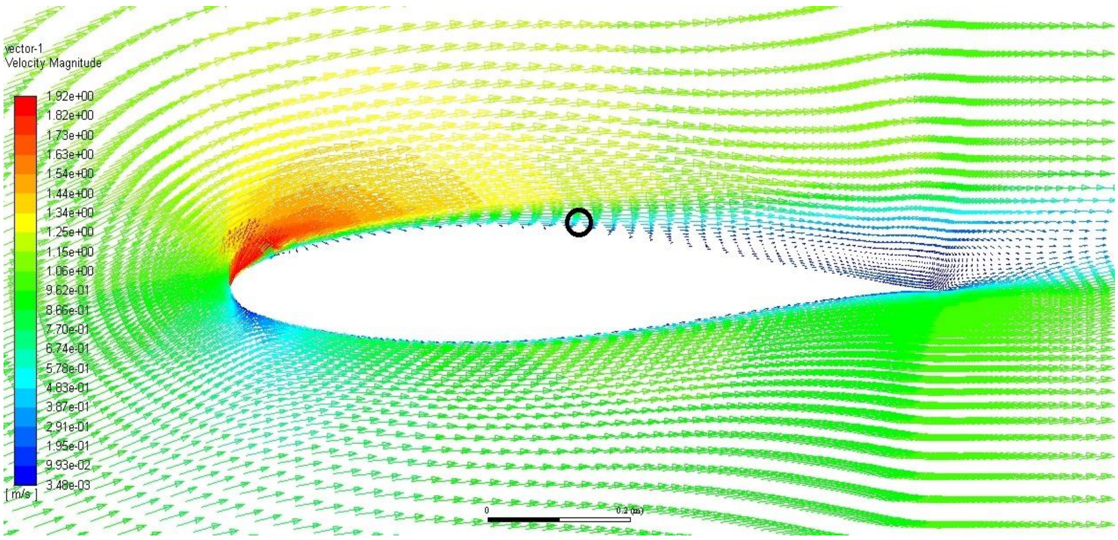

Figure 24. Velocity vector of NACA63-215 at 17^0 AoA

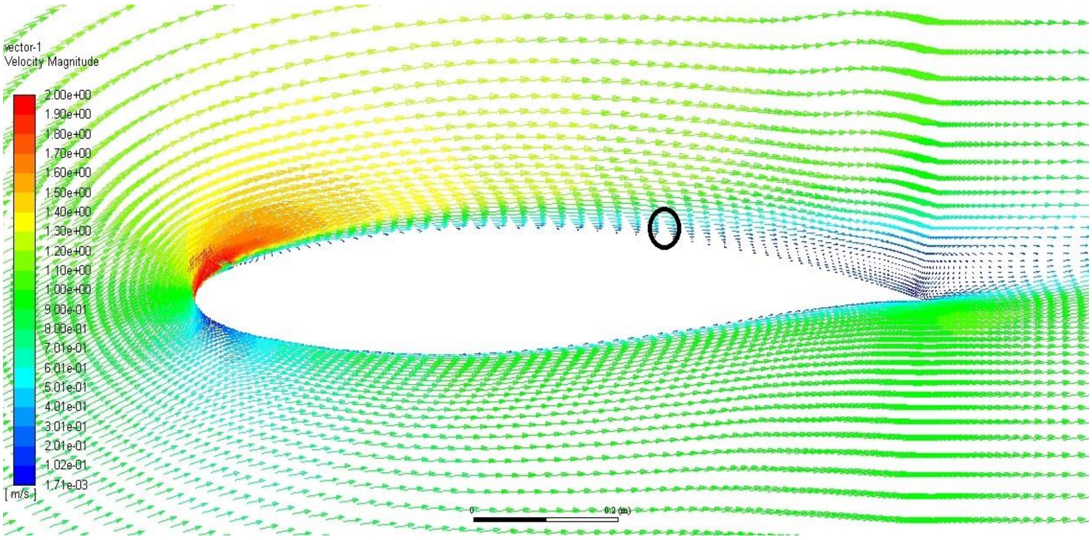

Figure 25. Velocity vector of NACA63-215_1 at 17^0 AoA

When Figures 24 and 25 were investigated it was seen that FS started at the nearly middle of the airfoil for NACA63-215 but FS started at the nearly back of the airfoil for NACA63-215_1 at 17^0 AoA.

The velocity vector of NACA63-215 and NACA63-215_1 at 21^0 AoA values were given in Figures 26 and 27 respectively.

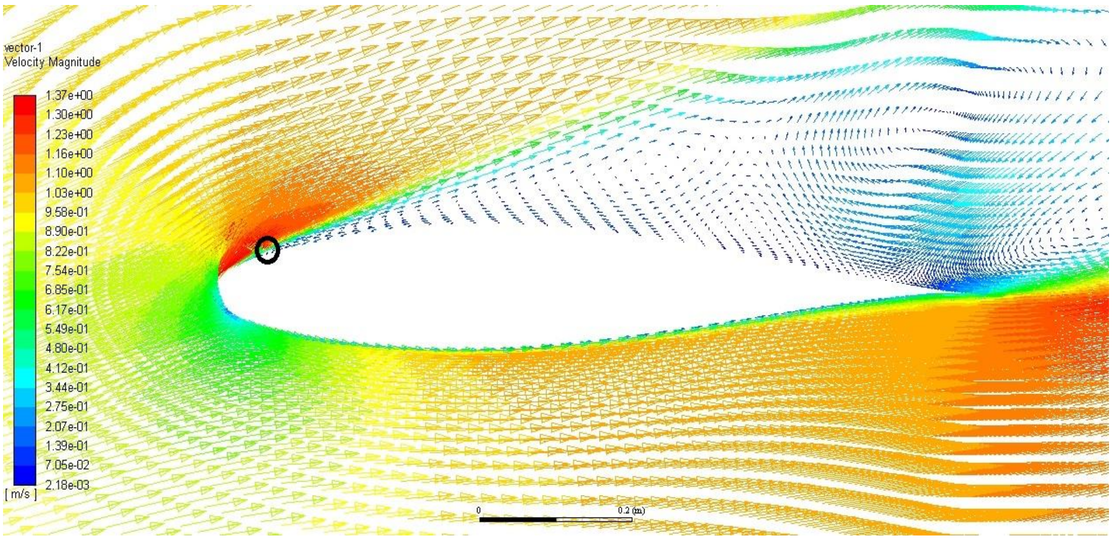

Figure 26. Velocity vector of NACA63-215 at 21^0 AoA

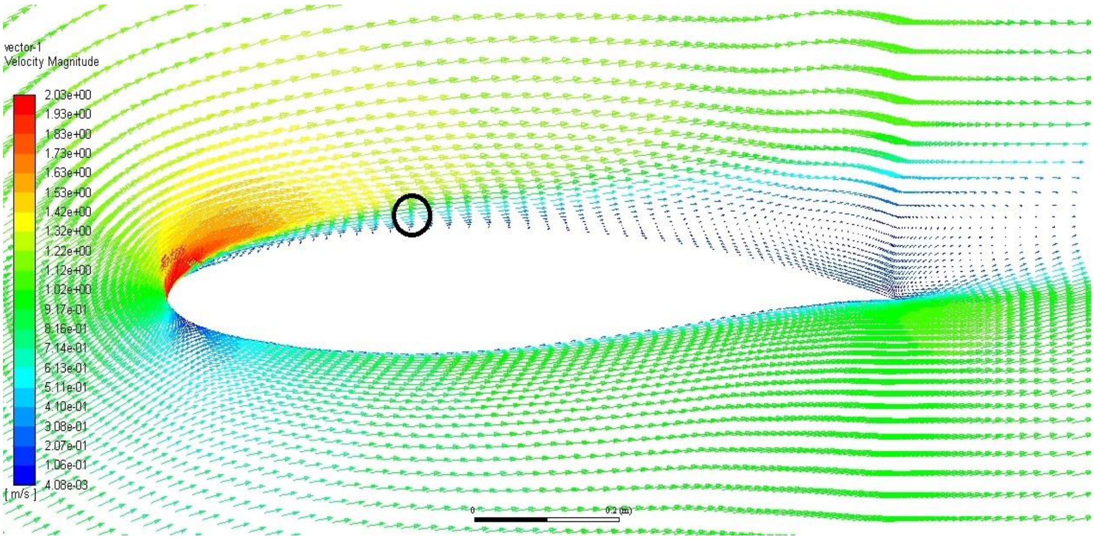

Figure 27. Velocity vector of NACA63-215_1 at 21^0 AoA

When Figures 26 and 27 were investigated it was seen that FS started at the front of the airfoil for NACA63-215 but FS started at the middle of the airfoil for NACA63-215_1 at 21^0 AoA.

Turbulent viscosity of NACA63-215 and NACA63-215_1 at 170 AoA values were given in Figures 28 and 29 respectively.

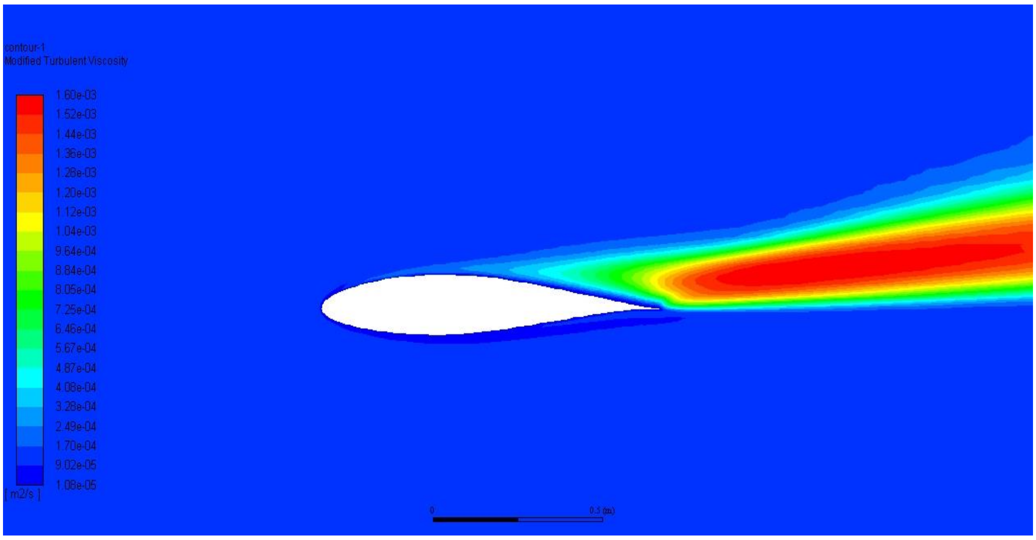

Figure 28. Turbulent viscosity of NACA63-215 at 17^0 AoA

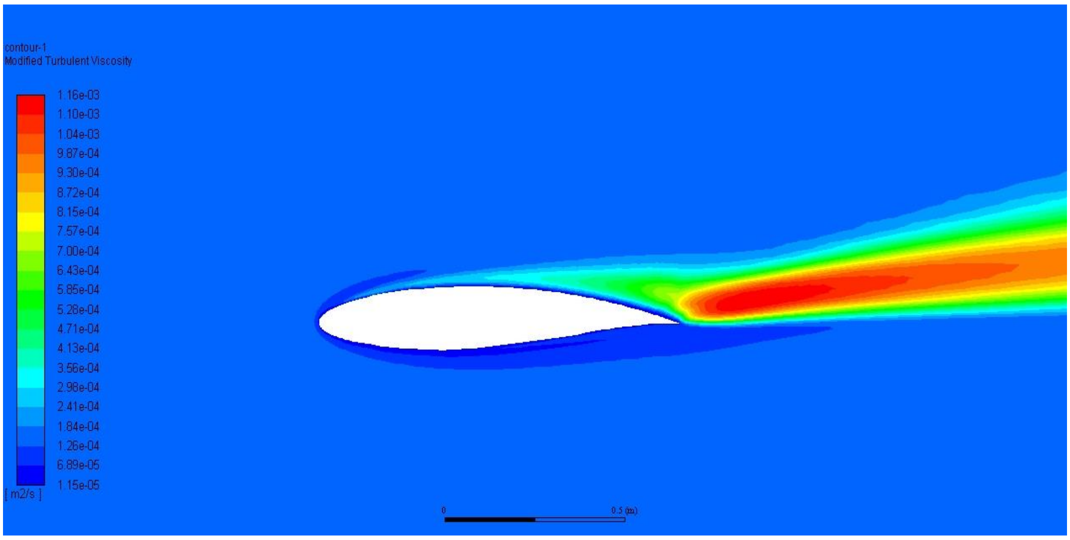

Figure 29. Turbulent viscosity of NACA63-215_1 at 17^0 AoA

After investigation of the analysis results, it was seen that the NACA63-215 airfoil should be used between 11^0-17^0 angle of attack, NACA63-215_1 should be used between 0^0-10^0, 18^0-23^0 angle of attack, to obtain maximum lift. So, different airfoils must be used during the flight to obtain the maximum lift as seen in figure 30.

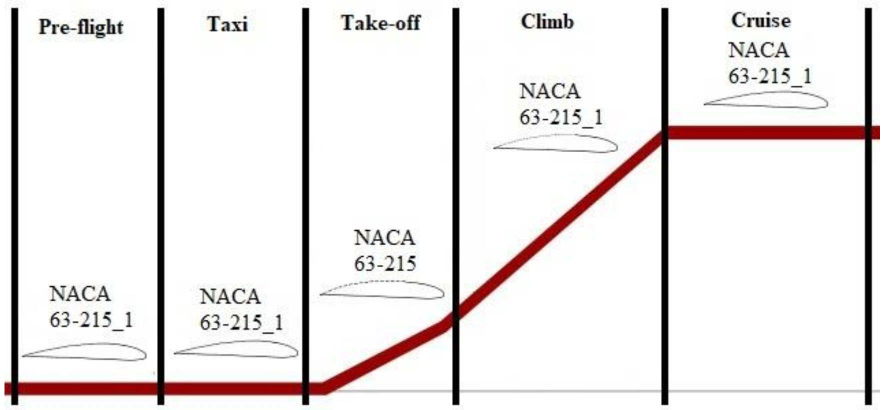

Figure 30. Usage of wing profile according to flight stages

4. RESULTS AND DISCUSSIONS

In this study, an improved airfoil was used to increase the AP of NACA63-215 at various angle of attack values. The AP of these 2-airfoils was compared in terms of the various angles of attack (between 0^0 and 23^0) values. Cd, Cl, and FS were used as performance parameters.

After the analysis, the comparison of the results was given below:

- Maximum Cl was obtained:
    - Between 11^0 and 17^0 AoA for original NACA63-215
    - Between 0^0 and 10^0, 18^0 and 23^0 AoA for NACA63-215_1
- There was no FS for three airfoils at 0^0 AoA.
- At 17^0 AoA, FS started:
    - at the middle of the airfoil for NACA63-215
    - at the back of the airfoil for NACA63-215_1
- Maximum AP was obtained on NACA63-215_1 nearly all AoA.
- Finally, the analysis results showed that it must be used different airfoils during the flight to obtain maximum lift.

REFERENCES

1. Chitte P, Jadhav PK, and Bansode SS., Statistic and dynamic analysis of typical wing structure of aircraft using Nastran, International Journal of Application or Innovation in Engineering & Management, 2, 7, 2013.
2. Doğru, M. H. 2017. Investigation of Velocity Distribution and Turbulent Energy for the Different Tip Shaped Projectiles. Çukurova University Journal of the Faculty of Engineering and Architecture, 32(3), 39-46.
3. Kevadiya M and Vaidya HA., 2D analysis of NACA 4412 airfoil, International Journal of Innovative Research in Science, Engineering and Technology, 2, 5,2013.
4. Petrilli J, Paul R, Gopalarathnam A, and Frink NT., A CFD Database for Airfoils and Wings at Post-Stall Angles of Attack, 31st AIAA Applied Aerodynamics Conference, Fluid Dynamics and Co-located Conferences, 2013.
5. Hossain S, Raiyan MF, Akanda MNU, and Jony NH., A comparative flow analysis of NACA 6409 and NACA 4412 aerofoil, International Journal of Research in Engineering and Technology, 03, 10, 2014.
6. Patel KS, Patel SB, Patel UB, and Ahuja AP., CFD analysis of an aerofoil, International Journal of Engineering Research, 3 (3), 154-158, 2014.
7. Triet NM, Viet NN, and Thang P M., Aerodynamic Analysis of Aircraft Wing, VNU Journal of Science: Mathematics – Physics, 31, 2, 2015.
8. Kavya G and Reddy BCR., Design and Finite Element Analysis of Aircraft Wing Using Ribs and Spars, International Journal & Magazine of Engineering Technology, Management and Research, 2, 11, 2015.
9. Kumar BSA, Ramalingaiah, Manjunath S, and Ganganna R., Computational Investigation of Flow Separation over Naca 23024 Airfoil at 6 Million Free Stream Reynolds Number, International Journal of Science, Technology and Society, 3, 6, 2015.
10. Göv İ and Korkmaz Ü., Comparison of Aerodynamic Performance of NACA 4412 and S809 Airfoil, International Mechanical Engineering and Technologies Conference, 183-188, 2016.
11. Göv, I., Dogru, M. H., & Korkmaz, U. 2019. Improvement of the aerodynamic performance of NACA 4412 using the adjustable airfoil profile

during the flight. Journal of The Faculty of Engineering and Architecture of Gazi University, 34(2), 1110-1125.

12. Korkmaz Ü. Design of Adjustable Airfoil to Delay Stall [M.S. thesis], The Institute for Graduate Studies in Natural and Applied Sciences, Gaziantep University 2018.

13. Korkmaz Ü, Göv İ, Doğru MH. 2020. Aerodynamic Analyses of Naca 63-215. The International Journal of Energy and Engineering Sciences, 5 (2), 156-166

14. Göv İ, Doğru MH. 2020. Aerodynamic Optimization of Naca 0012 Airfoil. The International Journal of Energy and Engineering Sciences, 5 (2), 146-155

15. Thibert JJ, Reneaux J, Moens F, and Priest J., ONERA activities on high lift devices for transport aircraft, Aeronautical Journal, 99, 395–411, 1995.

16. Spalart, P. R. and Allmaras, S.R., A One-Equation Turbulence Model for Aerodynamic Flows. Recherche Aerospatiale, 1, 5-21, 1994. http://airfoiltools.com/polar/details?polar=xf-n63215-il-50000-n5, 2020.